LWT - Food Science and Technology 85 (2017) 121–128

Contents lists available at ScienceDirect

LWT - Food Science and Technology

journal homepage: www.elsevier.com/locate/lwt

Effect of the espina corona gum on caseinate acid-induced gels

Débora N. López [a], Micaela Galante [a], Estela M. Alvarez [a], Patricia H. Risso [a, b, c], Valeria Boeris [a, d, *]

[a] Departamento de Química-Física, Facultad de Ciencias Bioquímicas y Farmacéuticas, Universidad Nacional de Rosario (UNR), Suipacha 531, 2000 Rosario, Argentina
[b] Facultad de Ciencias Veterinarias, Universidad Nacional de Rosario (UNR), Ovidio Lagos y Ruta 33, 2170 Casilda, Argentina
[c] Instituto de Física Rosario (IFIR, CONICET-UNR), 27 de Febrero 210 Bis, 2000 Rosario, Argentina
[d] Pontifica Universidad Católica Argentina, Pellegrini 3314, 2000 Rosario, Argentina

ARTICLE INFO

Article history:
Received 15 December 2016
Received in revised form
5 July 2017
Accepted 10 July 2017
Available online 11 July 2017

Keywords:
Sodium caseinate
Espina corona gum
Caseinate aggregation
Acid-induced gels

ABSTRACT

Espina corona gum (ECG) is a galactomannan extracted from the seeds of a leguminous tree native to America. In spite of its potential application in the food industry, casein protein aggregation and gelation in systems containing this gum have not yet been characterized. Here, the effect of ECG on the aggregation and gelation of sodium caseinate (NaCAS) and on the microstructure, the mechanical properties and color of acid-induced gels were studied. The aggregation process of NaCAS was studied in the presence of calcium, sucrose and ECG. ECG caused an increase in the aggregation time, without modification of the aggregation pH. The presence of calcium produced an increase in the aggregation pH due to the neutralization of the negative charges of the protein surface, resulting in a decrease in the aggregation time. However, the time required for NaCAS gelification was not affected by the presence of ECG. NaCAS/ECG mixed gels presented different color, water holding capacity and mechanical properties compared to NaCAS gels in the absence of ECG. Moreover, the presence of ECG produced differences in the microstructure of the acid-induced NaCAS gels.

1. Introduction

Many non-protein ingredients, including hydrocolloids, are added to food products in order to modify their texture and mechanical properties, as well as to ensure product stability (Pang, Deeth, Sharma, & Bansal, 2015b). Espina corona gum (ECG) is a galactomannan extracted from the seeds of a leguminous tree, *Gleditsia amorphoides*, which grows in America. It is a non-gelling polysaccharide used in food manufacture as thickener and stabilizer with potentially similar technological characteristics to locust bean gum (Pavón, Lazzaroni, Sabbag, & Rozycki, 2014; Perduca et al., 2013; Spotti, Santiago, Rubiolo, & Carrara, 2012a). Moreover, it has been reported that ECG has a similar manonose/galactose ratio to guar gum, a galactomannan of utmost importance in the food industry (Pavón et al., 2014).

Many dairy products are multi-component mixtures which contain a gelling biopolymer (de Jong & van de Velde, 2007). In particular, sodium caseinate (NaCAS) is a gelling milk protein widely used in food manufacture (Kinsella & Morr, 1984).

Acidification of an unfolded protein solution first leads to protein aggregation. Association among these protein aggregates results in protein gelation, when the amount of aggregated protein exceeds a critical concentration. Protein gel properties depend strongly on the structure of the protein aggregates and their association into a three-dimensional network (Maltais, Remondetto, & Subirade, 2008). As a consequence, the study of protein aggregation in diluted systems is important to understand how protein gelation takes place and to control rheological and physical properties of acid gels (Pachekrepapol, Horne, & Lucey, 2015).

Acidification of NaCAS has been traditionally induced by microbial fermentation. However, the chemical method of hydrolysis of glucono-δ-lactone (GDL) into gluconic acid has been increasingly used in laboratory-based studies due to its reproducibility and convenience (Braga, Menossi, & Cunha, 2006; Koh, Merino, & Dickinson, 2002). Moreover, these gels are usually useful to compare their physical properties with those of fermented products (Pang et al., 2015b). It is possible to change the acidification

* Corresponding author. Departamento de Química-Física, Facultad de Ciencias Bioquímicas y Farmacéuticas, Universidad Nacional de Rosario (UNR), Suipacha 531, 2000 Rosario, Argentina.
E-mail address: valeriaboeris@conicet.gov.ar (V. Boeris).

http://dx.doi.org/10.1016/j.lwt.2017.07.013
0023-6438/

rate by modifying the amount of GDL or the temperature (Braga, Menossi, & Cunha, 2006; de Kruif, 1997; Takeuchi & Cunha, 2008). In addition, many studies have used GDL to demonstrate that conditions of aggregation, gelification (pH, time) and also gel properties depend on the acidification rate (Jacob, Nöbel, Jaros, & Rohm, 2011; Kim & Kinsella, 1989).

Phase-separated networks are usually formed in food biopolymer mixtures (Morris & Wilde, 1997). In systems composed by more than one biopolymer, the final microstructure of acid-induced gels is not only influenced by the kinetics of gel formation but also by the kinetics of phase separation. The relative kinetics of these two processes has a profound influence on the texture and flavor properties of many food products (Doublier, Garnier, Renard, & Sanchez, 2000) (Norton & Frith, 2003). In particular, milk protein gelation induced by GDL has been used to kinetically trap a phase-separating system into different mixed gel structures (Aichinger et al., 2007). NaCAS and ECG aqueous systems are known to phase separate, being the phase separation process dependent on temperature, time and biopolymer concentration (López, Galante, Alvarez, Risso, & Boeris, 2017). Milk protein gelation has already been reported in the presence of a wide variety of galactomannans (Hidalgo et al., 2014b; Perrechil, Braga, & Cunha, 2009). A recent study reports the addition of ECG in cholesterol-reduced probiotic yoghurts, in which this galactomannan turned out to be the most influential variable in the preservation of sensory descriptors during storage. Moreover, we have recently published an article about the physicochemical study of aqueous mixed systems composed by ECG and NaCAS (López et al., 2017). Nonetheless, the effect of ECG on the gelation of milk proteins has not yet been elucidated and could be an important tool for the food industry to develop dairy products with innovative characteristics.

The aim of this work was to study the effect of ECG on the aggregation and gelation of NaCAS and the physical characteristics of the derived acid-induced gels, as model systems for acid dairy desserts.

2. Materials and methods

2.1. Materials

Bovine sodium caseinate (NaCAS), glucono-δ-lactone (GDL) and Rodamine B were purchased from Sigma-Aldrich (Steinheim, Germany). ECG was kindly donated by Idea Supply Argentina S.A. (Chaco, Argentine), and was used without further purification. A small amount of sodium azide, purchased from Mallinckrodt Chemical, (St. Louis, USA) was added to protein and polysaccharide suspensions in order to inhibit microbial development.

2.2. NaCAS acid aggregation

The time course of average size NaCAS particles during acid aggregation was studied in diluted systems through the dependence of turbidity (τ) on the wavelength (λ), according to Lombardi et al. (2016). The β parameter, related to the mean size of the aggregates (Hidalgo et al., 2011, pp. 199–222; Risso, Relling, Armesto, Pires, & Gatti, 2007), changes during the aggregation process and was obtained from the slope of log τ vs. log λ plots, according to Equation (1) (Holt, Parker, & Dalgleish, 1975):

$$\beta = 4.2 + \delta \log \tau / \delta \log \lambda \quad (1)$$

The acid aggregation of NaCAS 0.1 g/L was initiated by adding GDL, maintaining the ratio [GDL]/[NaCAS] (R) constant at 0.5.

Food products are multi-component systems in which proteins and polysaccharides are almost always present. Moreover, calcium is often added in acid dairy desserts. Thus, NaCAS acid-induced aggregation parameters were studied in the presence of ECG, calcium and sucrose. The concentrations studied were: $CaCl_2$ 0, 5 and 10 mM; sucrose 0, 5 and 10 g/L and ECG 0; 0.5 and 0.1 g/L. During acidification, pH values and absorption spectra (from 450 to 650 nm) were registered with a diode array detector every minute at 35 °C, in a Spekol 1200 spectrophotometer (Germany). The calculation of the β value at different times was performed. The parameters determined for the acid-induced aggregation were: aggregation time (A_t), aggregation pH (ApH) and final β value (FB).

2.3. Viscosity determinations: effect of ECG on the acid gelation of NaCAS

The effect of ECG on the acid gelation process of NaCAS was monitored by viscosity measurements. In order to ensure that NaCAS protein aggregates exceeded the critical value required for gelation to take place, NaCAS and NaCAS/ECG mixed systems were prepared at high biopolymer concentrations. The gelation process started after the addition of solid GDL, (R = 0.5). pH and apparent viscosity (η) of NaCAS (30 g/L) with the addition of ECG (in the range 0–3 g/L) were recorded every minute at 35 °C. Apparent viscosity values were measured during gelation at a fixed shear rate of 10 s^{-1}. A rotational viscometer Brookfield LVDV-II$^+$CP (USA) was used in steady shear with a cone-plate geometry (diameter 48 mm, angle 0.8°).

2.4. Preparation of NaCAS acid-induced gels

Gels were prepared from NaCAS aqueous solutions in the absence or presence of ECG in such a way as to obtain samples with a final concentration of 30 g/L and 1–3 g/L, respectively. Acid-induced gels were obtained by acidification of NaCAS systems with solid GDL added at 15 g/L, (R = 0.5) Systems were kept at 35 °C for 1 h to ensure gel formation.

2.5. Color digital analysis

The effect of the addition of ECG on the color of NaCAS gels was determined using a simple digital imaging method, based on the L*a*b* international standard model for color measurement. This model consists of a luminance or lightness (L*) component, ranging from 0 to 100, and two chromatic components: the a* component (from green to red) and the b* component (from blue to yellow), both ranging from −120 to +120 (Yam & Papadakis, 2004).

NaCAS gels were prepared according to Section 2.4 and they were photographed on a matte black background in a wooden box. A digital camera (Canon EOS-Rebel T3) was used in manual mode, with a lens aperture at f = 8, time of exposition 1/200, zoom 35 mm, no flash, ISO sensibility 400 and maximum resolution (3648 × 2736 pixels). Same conditions were used to photograph an IT8 calibration card (Wolf Faust, Frankfurt, Germany), in order to obtain a color profile. All images were stored in RAW formats. The graphic software Photoshop (Adobe Systems, Inc., San Jose, CA, USA) was used to determine the average values of the luminous and chromatic components, which were then converted into L*, a* and b* (Soazo, Pérez, Rubiolo, & Verdini, 2015). The whiteness index (WI) of NaCAS/ECG acid-induced gels was calculated according to Equation (2) (Salcedo-Chávez, Osuna-Castro, Guevara-Lara, Domínguez-Domínguez, & Paredes-López, 2002):

$$WI = L* - 3b* \quad (2)$$

WI quantifies the attribute by which an object is judged to approach white color (high WI values) instead of a yellowish tonality.

2.6. Water holding capacity

There are a wide number of reports that include the determination of WHC of gels using different conditions (Braga et al., 2006; Kruif, Anema, Zhu, Havea, & Coker, 2015; Pang, Deeth, & Bansal, 2015a; Serra, Trujillo, Quevedo, Guamis, & Ferragut, 2007; Ünal, Metin, & Işıklı, 2003). Water holding capacity (WHC) was determined by using the method described by Pang et al. (2015b). Five grams of acid-induced gels were prepared in plastic tubes as explained in Section 2.4 and were then centrifuged at 200 g for 10 min. Serum expelled was then weighed in order to calculate WHC. The experimental conditions used in our work were useful to determine the effect of ECG on the capacity of the gels to retain water in their structure without modifying their integrity.

2.7. Penetrometer profiles

Fifteen grams of gels were prepared according to Section 2.4 in 0.03 m high and 0.03 m wide cylindrical containers. Penetrometry was performed at room temperature using a Multitest 2.5-d (Mecmesin, Spain), with a 25 N load cell. The probe used was cylindrical with a plate base of 0.02 m diameter; operating at a speed of 1×10^{-3} m/s. Five independent replicates were performed. From the force-time curves, two mechanical parameters were obtained: fracture force (N), defined as the force at the first significant break, and the firmness (N/m), defined as the initial slope of the penetration curve (Pang et al., 2015b). The distance at which the gel broke was also determined.

2.8. Confocal laser scanning microscopy and image analysis

Microscopic techniques and image analyses provide an important tool for the characterization of protein gels (Ingrassia et al., 2013). Microstructural changes in the acid-induced NaCAS gels due to the presence of ECG were monitored by confocal laser scanning microscopy.

NaCAS was prepared at a final concentration of 30 g/L from dissolution of the commercial drug in a solution of the fluorescent protein label Rodamine B (0.02 g/L). This NaCAS solution was used to prepare acid-induced gels, as described in Section 2.4. The excitation used to induce fluorescence was performed using a laser light with a wavelength of 488 nm. Fluorescent emission was recorded at a wavelength of 568 nm. Gels were observed with an oil immersion objective of 60× using a confocal microscope (Nikon Eclipse TE-2000-E). Images were acquired with a pixel resolution of 1024 × 1024 using the EZ-C1 software designed by Nikon and were transformed to 8-bit type images and processed in order to obtain texture parameters by using specific programs. Four of the most significant image texture parameters were used in this work: Variance, Shannon entropy (SE), Uniformity (U) (Ingrassia et al., 2013) and Homogeneity or angular second moment (H) (Zheng, Sun, & Zheng, 2006). Moreover, the distribution of the diameter of the pores and the protein aggregates were determined through Image J (Version 1.485) software, using the Bone J plugin (Doube et al., 2010).

2.9. Statistical analysis

All determinations were performed at least in duplicate and the results were expressed as the media value with the associated uncertainty (standard deviation). Differences were considered significant when $p < 0.05$.

ANOVA was used to analyze significant factors affecting the NaCAS acid-induced aggregation. The assayed factors were ECG, calcium and sucrose concentrations that were tested at three levels in all the possible combinations. Aggregation time (A_t), aggregation pH (ApH) and final β value (FB) were the response variables studied. Mathematical equations were obtained by fitting the data, in order to estimate the effect of the studied factors on the response variables. In addition, the effect of these cosolutes on the acidification rate was also assessed by ANOVA.

3. Results and discussion

3.1. NaCAS acid aggregation

Fig. 1 shows the evolution of the β value as a function of pH and time for the NaCAS aggregation.

Three defined stages may be noticed. The first is when the acid aggregation process begins; the β parameter slightly decreases until it reaches a point when a sharp increase in the value of β is observed. The time required to reach this point is referred to as aggregation time (A_t) and indicates the time after which the system becomes unstable. Moreover, the pH value at this moment is defined as aggregation pH (ApH). In the second stage, the aggregates start to increase their size with the consequent increase in β parameter (Hidalgo et al., 2014a). In the third stage, upon aggregation, β tends towards an asymptotic value that was referred to as the final β value (FB), which enables us to compare the size of the aggregates at the end of the aggregation process under different conditions. This profile was observed in all the systems assayed.

In order to understand the results, it is important to highlight that two of the assayed cosolutes affected the acidification rate during the aggregation process ($p = 0.0102$): both Ca^{2+} and ECG decreased the velocity of acidification. This means that the decrease in pH in systems containing higher amounts of ECG or Ca^{2+} was slower than in those containing lower concentrations of these cosolutes. Nevertheless, the study of the effect of ECG on the acidification rate is beyond the scope of this work.

The study of the acid aggregation of NaCAS in the presence of cosolutes showed that only the calcium concentration was statistically significant for ApH ($p = 0.0451$). Equation (3) shows the mathematical model for this variable:

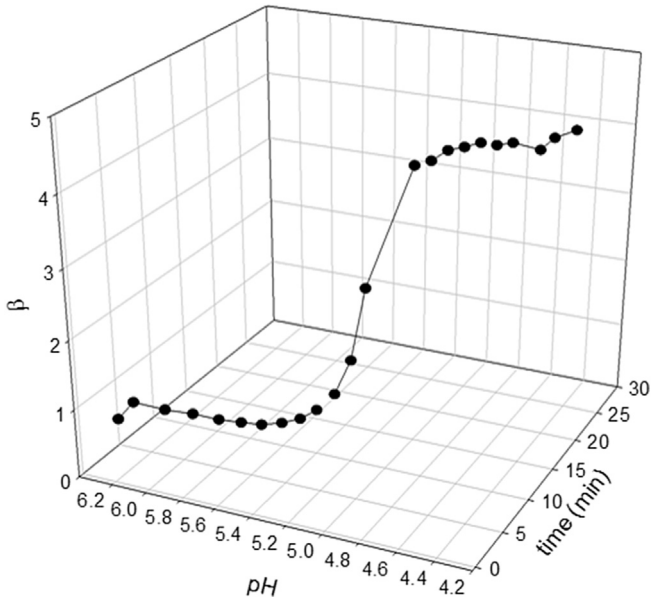

Fig. 1. Time course of the β parameter during the acidification process of NaCAS at 35 °C.

$$ApH = 4.91 + 0.028*\left[Ca^{2+}\right] \quad (3)$$

The aggregation process, which consists on the removal of the electrostatic repulsion due to the negative surface charges of NaCAS, was carried out by the addition of protons as a result of GDL hydrolysis into gluconic acid. While aggregation was in progress, there was a decrease in the pH until the equilibrium gluconate/gluconic acid was established. The presence of calcium contributed to neutralize the negative surface charge, so the pH at which aggregation began increased as the calcium concentration increased. The effect of the calcium concentration was also noticeable at the initial pH of the systems, being lower for those systems containing higher amounts of Ca^{2+} ($p < 0.0001$).

It is important to highlight that the pH obtained at the end of the acid aggregation process was similar in all the cases studied since it only depends on the amount of GDL added (Braga et al., 2006).

ECG did not cause any effect on ApH, suggesting that its presence did not change the net amount of protonable groups exposed by NaCAS.

Calcium concentration was statistically significant for A_t ($p = 0.0441$), negatively affecting this value, as shown in Equation (4).

$$At^{-1} = 0.19 + 9.3.10^{-3}*\left[Ca^{2+}\right] - 1.06*[ECG] \quad (4)$$

As it was previously discussed for the ApH, this effect may be caused by the net positive charge of calcium, which considerably reduces the electrostatic stability of NaCAS particles, making them unstable and resulting in a faster aggregation process. Moreover, it has been reported that the addition of calcium to NaCAS could lead to the formation of small colloidal particles. In agreement with this, the protein aggregates have a more compact structure at the initial state, which drives the acid aggregation process further (Alvarez, Risso, Gatti, Burgos, & Sala, 2007; Mancilla Canales, Hidalgo, Risso, & Alvarez, 2010). This is in accordance with the higher β values obtained under the mentioned conditions before the addition of GDL.

Although ECG did not affect ApH, the increase in the ECG concentration produced an increase in A_t ($p = 0.0131$), as shown in Equation (4). This effect may be explained considering the fact that ECG affected the acidification rate, making larger the time required to reach the ApH as the ECG concentration increased. As it was pointed out in the introduction, the pH at which the aggregation/gelification takes place depends on the acidification rate; however, in this case, the ApH was not affected by the addition of ECG. Even if the presence of ECG modified the acidification rate, it was not enough to modify the ApH.

Previous reports corroborate the correlation between the β value and the hydrodynamic diameter of the protein aggregates (Hidalgo et al., 2011, pp. 199–222; Risso et al., 2007). FB of the protein aggregates formed at the end of the aggregation process was only significantly affected by the ECG concentration ($p = 0.0194$) (Equation (5)).

$$FB = 3.9 + 150*[ECG]^2 \quad (5)$$

This suggests that the protein aggregates obtained after the acid aggregation process are higher in the presence of ECG. As previously reported (Ouanezar, Guyomarc'h, & Bouchoux, 2012), after the first step of aggregation process takes place, there is a rearrangement of the protein particles, which leads to changes in the aggregate structure and involves mainly hydrophobic interactions.

Sucrose was not statistically significant for any of the studied parameters ($p > 0.05$).

3.2. Effect of ECG on the acid gelation of NaCAS

Fig. 2 shows the evolution of the apparent viscosity of NaCAS and NaCAS/ECG mixed systems during acid gelation. In this case, the ECG had no effect on the acidification rate, probably due to the increased GDL/ECG ratio, compared to that used in the aggregation assays. As acidification was being carried out, the apparent viscosity slightly decreased during the first 20 min. Then, as shown in Fig. 2, there was a sharp increase in the apparent viscosity of the systems when the pH moved closer to the isoelectric pH of NaCAS, signaling the sol-gel transition.

Although ECG affected the A_t in diluted systems, ECG had no significant effect on gelation time ($p = 0.885$), since gel formation was complete at (22 ± 1) min in all the systems studied. The pH value at which gels were formed was 5.00 ± 0.02 and was not influenced by the addition of ECG, which is in agreement with the results obtained for aggregation in diluted systems.

3.3. Color digital analysis

As ECG is a slightly yellowish powder, its presence in the mixed gels is expected to produce some kind of color alteration. The effect of ECG on the lightness and chromatic components as well as on the whiteness index of NaCAS acid-induced gels is shown in Table 1. The L^* of the acid gels was not significantly affected by the presence of ECG; however, both chromatic components increased when ECG concentration was 2 g/L or 3 g/L. Moreover, the addition of ECG did not affect the WI of NaCAS acid-induced gels when ECG was present at 1 g/L. However, higher polysaccharide concentrations resulted in a decrease in the WI. This could be related not only to the color of the ECG but also to changes in the gel structure that affected the perception of these gel systems.

3.4. Water holding capacity

Table 2 shows the WHC of NaCAS acid-induced gels in the presence of increasing concentrations of ECG (0–3 g/L). It is to be noted that the gels containing ECG presented lower WHC. The effect of the addition of guar gum on the WHC of acid milk gels with

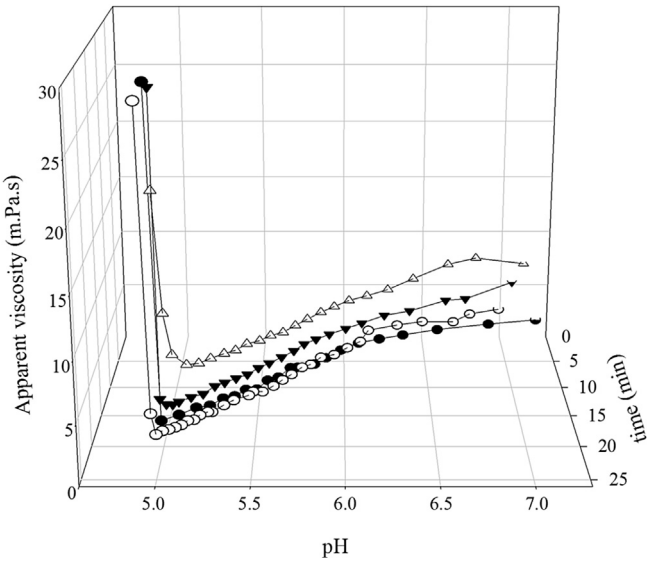

Fig. 2. Effect of ECG on apparent viscosity during the acid-gelation process of NaCAS. (●) without ECG (○) with 1 g/L ECG (▼) with 2 g/L ECG (Δ) with 3 g/L ECG. (NaCAS 30 g/L, GDL 15 g/L, Temperature 35 °C).

Table 1
Color digital analysis of NaCAS acid-induced gels in the presence of ECG. (NaCAS 30 g/L, GDL 15 g/L, Temperature 35 °C).

ECG (g/L)	L*	a*	b*	WI
0	95 ± 1	2.8 ± 0.7	14 ± 1	52 ± 2
1	95.7 ± 0.5	2.8 ± 0.6	15 ± 1	51 ± 2
2	95 ± 1	3.7 ± 0.7	17 ± 1	45 ± 2
3	94 ± 1	3.7 ± 0.8	17 ± 1	43 ± 2

L* = lightness; a* = red-green color; b* = yellow-blue color; WI= Whiteness index.

Table 2
Effect of ECG on the water holding capacity and texture parameters of NaCAS acid-induced gels. (NaCAS 30 g/L, GDL 15 g/L, Temperature 35 °C).

ECG (g/L)	WHC (%)	SE	U	H
0	84.7 ± 0.5	3.7 ± 0.3	0.19 ± 0.06	0.33 ± 0.04
1	72 ± 2	4.50 ± 0.06	0.072 ± 0.004	0.042 ± 0.004
2	69.5 ± 0.9	4.3 ± 0.1	0.09 ± 0.02	0.09 ± 0.02
3	51.9 ± 0.4	4.8 ± 0.1	0.06 ± 0.01	0.04 ± 0.02

WHC = water holding capacity; SE= Shannon entropy; U= Uniformity; H= Homogeneity.

similar results has already been reported by Pang et al. (2015a). This negative effect may be attributed to a phase separation through a depletion-flocculation mechanism. ECG could be forming a viscous continuous phase containing trapped compact protein aggregates, resulting in a reduced WHC (Everett & McLeod, 2005).

3.5. Penetrometer profiles

The representative penetrometer profiles of the NaCAS acid-induced gels containing different concentrations of ECG are shown in Fig. 3A, and the values of the firmness, the fracture force and the distance at which the gel fractured are shown in Fig. 3B.

The penetrometer profile of the NaCAS acid-induced gels in the absence of ECG reveals that the force required to fracture the gel is low compared to the force required to fracture WPI gels. However, both the values of force at fracture and firmness are similar to those obtained by acid induced skim milk gels, indicating that the strength of the NaCAS acid-induced gel, is moderate and similar to skim milk gels (Pang et al., 2015b).

Gels added with ECG 1 g/L showed a similar penetrometer profile to those obtained for the NaCAS gels in the absence of ECG. Although firmness was not affected; the gel broke at a lower deformation rate than it did in the absence of ECG, the fracture force being also lower. On the other hand, the addition of 2 g/L ECG produced less firm gels that fracture at lesser penetration, thus being less deformable. The decrease in the distance at break was also reported for WPI gels when they were added with ECG (Spotti et al., 2012a). The particular aspect of these gels is that after the fracture point, there was some kind of cohesive structure that still remained, as can be inferred from the fact that the force after breaking point did not decrease abruptly.

The presence of the highest ECG concentration (3 g/L) dramatically affected the mechanical properties of the system, reducing firmness significantly and making it impossible to determine the fracture point. This could be explained by the fact that the viscous behavior of this acidified NaCAS/ECG system dominates over the elastic behavior, thus forming a weak mesh.

3.6. Confocal laser scanning microscopy (CLSM) and image processing

3.6.1. Microstructure of NaCAS/ECG acid gels

The microstructure of acid-induced NaCAS/ECG gels visualized by CLSM is shown in Fig. 4. Protein appears as bright areas due to the Rodamine label, while the aqueous phase or pores correspond to the dark regions.

It is to be noted that the microstructure of these gels was highly affected by the presence of ECG. Spotti et al. (2012a) had previously reported that the microstructure of WPI gels was affected by the presence of ECG because the systems containing WPI and ECG phase-separate.

At this point, it is to be highlighted that when systems composed by 30 g/L NaCAS and ECG concentrations in the range of 1–3 g/L were incubated for 24 h at 35 °C (without acidification),

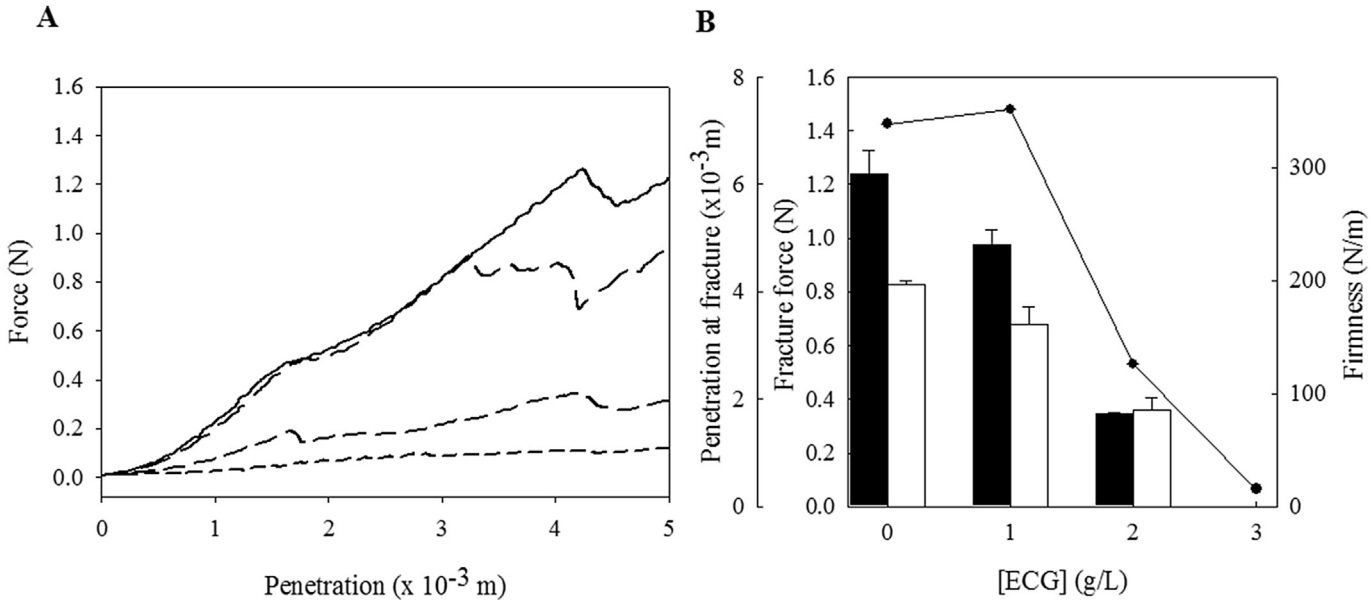

Fig. 3. A) Penetrometer profiles of NaCAS acid-induced gels in the presence of ECG (_____ 0 g/L ECG, __ __ __ 1 g/L ECG, _ _ _ 2 g/L ECG, —— 3 g/L ECG) (NaCAS 30 g/L, GDL 15 g/L. Temperature 35 °C). B) Effect of the ECG concentration on the penetrometry parameters of the NaCAS acid-induced gels. (NaCAS 30 g/L, GDL 15 g/L. Temperature 35 °C). White bars, black bars and dots correspond to the distance at fracture, fracture force and firmness, respectively.

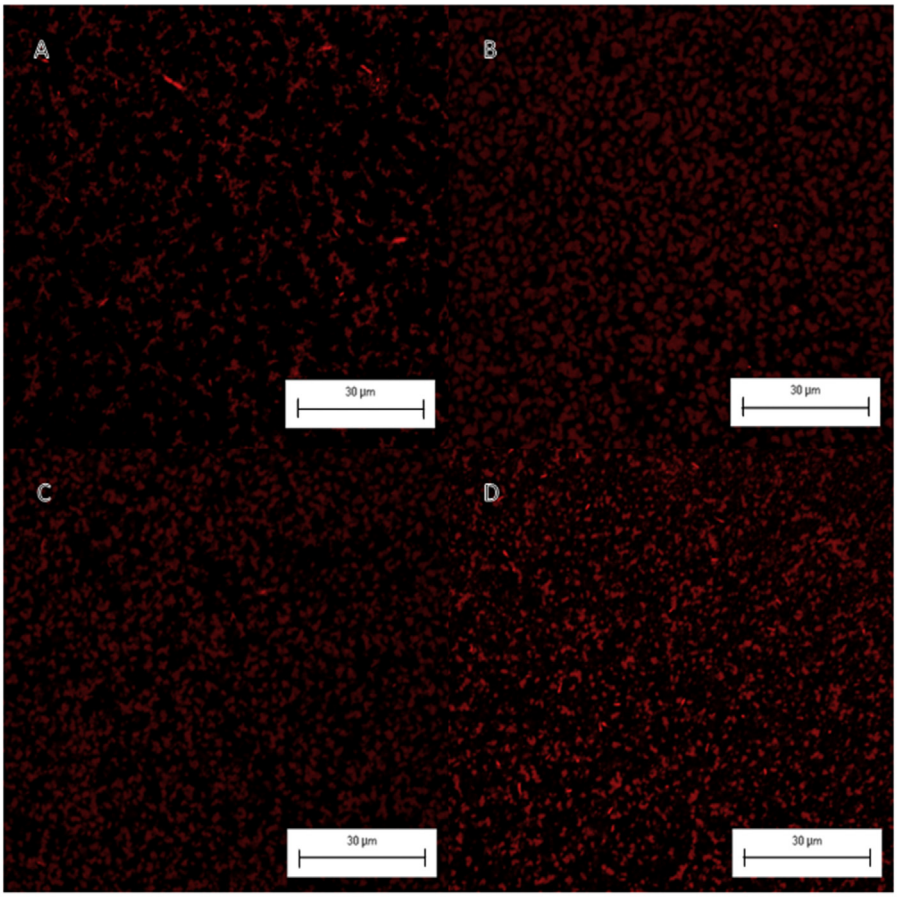

Fig. 4. Confocal laser scanning microscopy of acid-induced NaCAS gels A) without ECG. B), C) and D) with 1, 2 and 3 g/L ECG, respectively. (NaCAS 30 g/L, GDL 15 g/L. Temperature 35 °C). Scale bar = 15 µm.

they exhibited phase separation (López et al., 2017). Several authors state that the final microstructure of acid-induced gels is influenced not only by the kinetics of gel formation but also by the kinetics of phase separation between the two biopolymers of the system. The relative kinetics of these two processes is responsible for the final characteristics of these gels (Aichinger et al., 2007; Doublier et al., 2000; Norton & Frith, 2003).

It has been previously reported that acid-induced NaCAS/locust bean gum gels do not show macroscopic phase separation (Perrechil & Cunha, 2012; Perrechil et al., 2009). In the acid-induced NaCAS/ECG gels studied in this work, phase separation was not observed macroscopically, but could be estimated by image analysis.

Although the effect of ECG on the microstructure of the NaCAS acid-induced gels can be partially assessed by visual inspection of the CLSM images, some subtle differences cannot be distinguished by the human eye. Thus, it is important to study these gels through quantitative parameters obtained by means of digital analysis.

3.6.2. Texture digital analysis

The dimensionless texture parameters SE, U and H were obtained by image processing and are shown in Table 2.

Acid-induced NaCAS gels without ECG showed low U values and high SE values, in agreement with the observed structures consisting in particles dispersed throughout its volume. The addition of ECG in the acid gels caused an inversion in these parameters, resulting in higher U values and lower SE values. These parameters are related to the amount of each grey-level tone in the images; i.e, are based on the element's value. A high SE value with a low U value implies that there are several grey tonalities in the image. However, these parameters do not provide information about the spatial distribution of each one of these pixels. The parameters that give information about the spatial arrangement of the pixels in image are calculated based on the spatial position of each element, the H being one of these. Particularly, the H is inversely related to the amount of grey-tone transitions. Lower H values when ECG is added to the NaCAS gels are in accordance with heterogeneous structures, in which the particles are distributed in such a way that the image presents many grey-tone transitions.

The variance texture parameter was also calculated for each image obtained. This value increased in the NaCAS/ECG gels (from 950 ± 90 without ECG addition to 1400 ± 100 in the presence of 3 g/L ECG), indicating a higher degree of local variations in the structure of protein aggregates in the presence of the galactomannan. This is in agreement with the effect of ECG on the structure of NaCAS aggregates in solution, reported previously (López et al., 2017).

3.6.3. Size distribution of protein aggregates and pores

Size distribution of pores and protein aggregates in acid-induced NaCAS/ECG gels were estimated by image processing, and are shown in Fig. 5.

Polysaccharides added to casein dispersion are known to cause attractive interactions among the protein particles due to depletion effects (de Bont, van Kempen, & Vreeker, 2002). ECG has not a clear effect on the size distribution of the protein aggregates. However, the size of the pores in NaCAS acid-induced gels is smaller and their distribution is narrower in the presence of ECG, this effect being

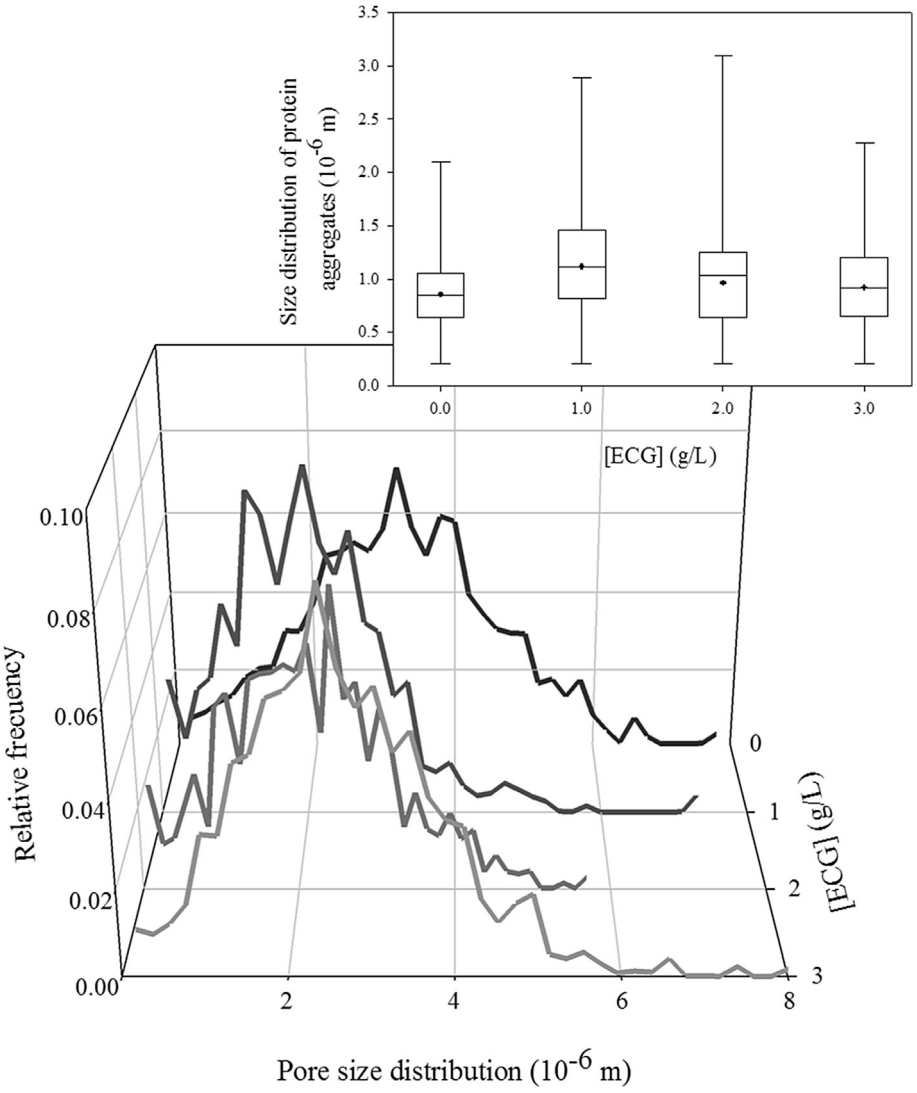

Fig. 5. Pore size distribution (main plot) and size distribution of protein aggregates (inset) in NaCAS/ECG acid-induced gels (NaCAS 30 g/L, GDL 15 g/L. Temperature 35 °C).

independent of the galactomannan concentration. This could be indicating that the protein network became more compact with a smaller pore size in the presence of ECG. As Pugnaloni, Matia-Merino, and Dickinson (2005) showed in NaCAS/sucrose gels, this may be due to the enhanced interconnectivity among protein particles. This interpretation is in agreement with the results obtained by the turbidimetric experiments during the acid aggregation of NaCAS (Equation (5)).

Several articles reveal that the pores of gels formed by phase-separating systems, composed by a gelling protein and a polysaccharide, are greater than the pores of gels formed in the absence of the polysaccharide (Çakır et al., 2012; Çakır & Foegeding, 2011; Sanchez, Zuniga-Lopez, Schmitt, Despond, & Hardy, 2000; Spotti Santiago, Rubiolo, & Carrara, 2012b). Although ECG-NaCAS systems are known to phase separate, our findings are not in agreement with these previous reports since the pores of the gels containing ECG are smaller than those in the absence of ECG. Matia-Merino, Lau, and Dickinson (2004) have reported a similar effect in micelles/pectin gels. They have proposed that the gelation process proceeded faster than the phase separation. The same phenomenon may have taken place in the NaCAS/ECG acid gels studied in this work.

4. Conclusions

Our previous findings, supported by the literature, suggest that ECG modifies the interaction of the NaCAS proteins with water and also the NaCAS-NaCAS interaction; ECG produces the flocculation of NaCAS by a depletion mechanism. In this work, the effect of ECG on the acid-induced aggregation and gelation of NaCAS was studied. Although the aggregation time of NaCAS was modified by the presence of ECG, the gelation time was not affected. NaCAS acid-induced gels resulted in smaller pores size and differential textural parameters in the presence of ECG. In addition, different concentrations of ECG modified significantly the appearance, texture and WHC of the studied gels.

Acknowledgements

This work was supported by grants from Universidad Nacional of Rosario, UNR (1BIO358), from Consejo Nacional de Investigaciones Científicas y Técnicas, CONICET, Argentina (PIP 2014–2016 GI) and from Agencia Nacional de Promoción Científica y Tecnológica (PICT 2011-1354). The authors would like to thank the English Area of Facultad of Ciencias Bioquímicas and

Farmacéuticas, UNR, for the language correction of the manuscript. We would also like to thank Julia Lombardi for advising us about image processing and Marina Soazo for the collaboration in the experimental work.

References

Aichinger, P.-A., Dillmann, M.-L., Rami-Shojaei, S., Paterson, A., Michel, M., & Horne, D. S. (2007). *Xanthan gum in skim milk: Designing structure into acid milk gels*.

Alvarez, E. M., Risso, P. H., Gatti, C. A., Burgos, M., & Sala, V. S. (2007). Calcium-induced aggregation of bovine caseins: Effect of phosphate and citrate. *Colloid and Polymer Science, 285*, 507–514.

de Bont, P. W., van Kempen, G. M. P., & Vreeker, R. (2002). Phase separation in milk protein and amylopectin mixtures. *Food Hydrocolloids, 16*, 127–138.

Braga, A., Menossi, M., & Cunha, R. L. (2006). The effect of the glucono-δ-lactone/caseinate ratio on sodium caseinate gelation. *International Dairy Journal, 16*, 389–398.

Çakır, E., Daubert, C. R., Drake, M. A., Vinyard, C. J., Essick, G., & Foegeding, E. A. (2012). The effect of microstructure on the sensory perception and textural characteristics of whey protein/κ-carrageenan mixed gels. *Food Hydrocolloids, 26*, 33–43.

Çakır, E., & Foegeding, E. A. (2011). Combining protein micro-phase separation and protein–polysaccharide segregative phase separation to produce gel structures. *Food Hydrocolloids, 25*, 1538–1546.

Doube, M., Kłosowski, M. M., Arganda-Carreras, I., Cordelières, F. P., Dougherty, R. P., & Jackson, J. S. (2010). BoneJ: Free and extensible bone image analysis in ImageJ. *Bone, 47*, 1076–1079.

Doublier, J.-L., Garnier, C., Renard, D., & Sanchez, C. (2000). Protein–polysaccharide interactions. *Current Opinion in Colloid & Interface Science, 5*, 202–214.

Everett, D. W., & McLeod, R. E. (2005). Interactions of polysaccharide stabilisers with casein aggregates in stirred skim-milk yoghurt. *International Dairy Journal, 15*, 1175–1183.

Hidalgo, M., Canales, M. M., Nespolo, C., Reggiardo, A., Alvarez, E., & Wagner, J. (2011). *Comparative study of bovine and ovine caseinate aggregation processes: Calcium-induced aggregation and acid aggregation*. New York: Protein Aggregation. Nova Publishers.

Hidalgo, M. E., Fontana, M., Armendariz, M., Riquelme, B., Wagner, J. R., & Risso, P. (2014a). Acid-induced aggregation and gelation of sodium caseinate-guar gum mixtures. *Food Biophysics*, 1–14.

Hidalgo, M. E., Fontana, M., Armendariz, M., Riquelme, B., Wagner, J. R., & Risso, P. (2014b). Acid-induced aggregation and gelation of sodium caseinate-guar gum mixtures. *Food Biophysics, 10*, 181–194.

Holt, C., Parker, T. G., & Dalgleish, D. G. (1975). Measurement of particle sizes by elastic and quasi-elastic light scattering. *Biochimica et Biophysica Acta (BBA) - Protein Structure, 400*, 283–292.

Ingrassia, R., Costa, J. P., Hidalgo, M. E., Canales, M. M., Castellini, H., & Riquelme, B. (2013). Application of a digital image procedure to evaluate microstructure of caseinate and soy protein acid gels. *LWT-food Science and Technology, 53*, 120–127.

Jacob, M., Nöbel, S., Jaros, D., & Rohm, H. (2011). Physical properties of acid milk gels: Acidification rate significantly interacts with cross-linking and heat treatment of milk. *Food Hydrocolloids, 25*, 928–934.

de Jong, S., & van de Velde, F. (2007). Charge density of polysaccharide controls microstructure and large deformation properties of mixed gels. *Food Hydrocolloids, 21*, 1172–1187.

Kim, B. Y., & Kinsella, J. E. (1989). Rheological changes during slow acid induced gelation of milk by d-glucono-δ-lactone. *Journal of Food Science, 54*, 894–898.

Kinsella, J. E., & Morr, C. V. (1984). Milk proteins: Physicochemical and functional properties. *Critical Reviews in Food Science & Nutrition, 21*, 197–262.

Koh, M. W. W., Merino, L. M., & Dickinson, E. (2002). Rheology of acid-induced sodium caseinate gels containing added gelatin. *Food Hydrocolloids, 16*, 619–623.

de Kruif, C. G. (1997). Skim milk acidification. *Journal of Colloid and Interface Science, 185*, 19–25.

Kruif, C. G. d., Anema, S. G., Zhu, C., Havea, P., & Coker, C. (2015). Water holding capacity and swelling of casein hydrogels. *Food Hydrocolloids, 44*, 372–379.

Lombardi, J., Spelzini, D., Corrêa, A. P. F., Brandelli, A., Risso, P., & Boeris, V. (2016). Milk protein suspensions enriched with three essential minerals: Physicochemical characterization and aggregation induced by a novel enzymatic pool. *Colloids and Surfaces B: Biointerfaces, 140*, 452–459.

López, D. N., Galante, M., Alvarez, E. M., Risso, P. H., & Boeris, V. (2017). Physicochemical study of mixed systems composed by bovine caseinate and the galactomannan from Gleditsia amorphoides. *Carbohydrate Polymers, 173*, 1–6.

Maltais, A., Remondetto, G. E., & Subirade, M. (2008). Mechanisms involved in the formation and structure of soya protein cold-set gels: A molecular and supramolecular investigation. *Food Hydrocolloids, 22*, 550–559.

Mancilla Canales, M. A., Hidalgo, M. a. E. ., Risso, P. H., & Alvarez, E. M. (2010). Colloidal stability of bovine calcium caseinate suspensions. Effect of protein concentration and the presence of sucrose and lactose. *Journal of Chemical and Engineering Data, 55*, 2550–2557.

Matia-Merino, L., Lau, K., & Dickinson, E. (2004). Effects of low-methoxyl amidated pectin and ionic calcium on rheology and microstructure of acid-induced sodium caseinate gels. *Food Hydrocolloids, 18*, 271–281.

Morris, V. J., & Wilde, P. J. (1997). Interactions of food biopolymers. *Current Opinion in Colloid & Interface Science, 2*, 567–572.

Norton, I., & Frith, W. (2003). Food colloids. Biopolymers and materials. *RSC: Cambridge*, 282–297.

Ouanezar, M., Guyomarc'h, F., & Bouchoux, A. (2012). AFM imaging of milk casein Micelles: Evidence for structural rearrangement upon acidification. *Langmuir, 28*, 4915–4919.

Pachekrepapol, U., Horne, D., & Lucey, J. (2015). Effect of dextran and dextran sulfate on the structural and rheological properties of model acid milk gels. *Journal of Dairy Science, 98*, 2843–2852.

Pang, Z., Deeth, H., & Bansal, N. (2015a). Effect of polysaccharides with different ionic charge on the rheological, microstructural and textural properties of acid milk gels. *Food Research International, 72*, 62–73.

Pang, Z., Deeth, H., Sharma, R., & Bansal, N. (2015b). Effect of addition of gelatin on the rheological and microstructural properties of acid milk protein gels. *Food Hydrocolloids, 43*, 340–351.

Pavón, Y. L., Lazzaroni, S. M., Sabbag, N. G., & Rozycki, S. D. (2014). Simultaneous effects of gelatin and espina corona gum on rheological, physical and sensory properties of cholesterol-reduced probiotic yoghurts. *International Journal of Food Science & Technology, 49*, 2245–2251.

Perduca, M. J., Spotti, M. J., Santiago, L. G., Judis, M. A., Rubiolo, A. C., & Carrara, C. R. (2013). Rheological characterization of the hydrocolloid from Gleditsia amorphoides seeds. *LWT-food Science and Technology, 51*, 143–147.

Perrechil, F., Braga, A., & Cunha, R. (2009). Interactions between sodium caseinate and LBG in acidified systems: Rheology and phase behavior. *Food Hydrocolloids, 23*, 2085–2093.

Perrechil, F., & Cunha, R. (2012). Development of multiple emulsions based on the repulsive interaction between sodium caseinate and LBG. *Food Hydrocolloids, 26*, 126–134.

Pugnaloni, L. A., Matia-Merino, L., & Dickinson, E. (2005). Microstructure of acid-induced caseinate gels containing sucrose: Quantification from confocal microscopy and image analysis. *Colloids and Surfaces B: Biointerfaces, 42*, 211–217.

Risso, P. H., Relling, V. M., Armesto, M. S., Pires, M. S., & Gatti, C. A. (2007). Effect of size, proteic composition, and heat treatment on the colloidal stability of proteolyzed bovine casein micelles. *Colloid and Polymer Science, 285*, 809–817.

Salcedo-Chávez, B., Osuna-Castro, J. A., Guevara-Lara, F., Domínguez-Domínguez, J., & Paredes-López, O. (2002). Optimization of the isoelectric precipitation method to obtain protein isolates from amaranth (Amaranthus cruentus) seeds. *Journal of Agricultural and Food Chemistry, 50*, 6515–6520.

Sanchez, C., Zuniga-Lopez, R., Schmitt, C., Despond, S., & Hardy, J. (2000). Microstructure of acid–induced skim milk–locust bean gum–xanthan gels. *International Dairy Journal, 10*, 199–212.

Serra, M., Trujillo, A. J., Quevedo, J. M., Guamis, B., & Ferragut, V. (2007). Acid coagulation properties and suitability for yogurt production of cows' milk treated by high-pressure homogenisation. *International Dairy Journal, 17*, 782–790.

Soazo, M., Pérez, L. M., Rubiolo, A. C., & Verdini, R. A. (2015). Prefreezing application of whey protein-based edible coating to maintain quality attributes of strawberries. *International Journal of Food Science & Technology, 50*, 605–611.

Spotti, M. J., Santiago, L. G., Rubiolo, A. C., & Carrara, C. R. (2012a). Mechanical and microstructural properties of milk whey protein/espina corona gum mixed gels. *LWT - Food Science and Technology, 48*, 69–74.

Spotti, M. J., Santiago, L. G., Rubiolo, A. C., & Carrara, C. R. (2012b). Mechanical and microstructural properties of milk whey protein/espina corona gum mixed gels. *LWT-food Science and Technology, 48*, 69–74.

Takeuchi, K. P., & Cunha, R. L. (2008). Influence of ageing time on sodium caseinate gelation induced by glucono-δ-lactone at different temperatures. *Dairy Science & Technology, 88*, 667–681.

Ünal, B., Metin, S., & Işıklı, N. D. (2003). Use of response surface methodology to describe the combined effect of storage time, locust bean gum and dry matter of milk on the physical properties of low-fat set yoghurt. *International Dairy Journal, 13*, 909–916.

Yam, K. L., & Papadakis, S. E. (2004). A simple digital imaging method for measuring and analyzing color of food surfaces. *Journal of Food Engineering, 61*, 137–142.

Zheng, C., Sun, D.-W., & Zheng, L. (2006). Recent applications of image texture for evaluation of food qualities—a review. *Trends in Food Science & Technology, 17*, 113–128.